CHAPTER 4

Photocatalytic Water Splitting Under Visible Light: Concept and Catalysts Development

R.M. Navarro*, **F. del Valle, J.A. Villoria de la Mano, M.C. Álvarez-Galván,** and **J.L.G. Fierro**

Contents

1. INTRODUCTION

Sunlight in the near-infrared, visible, and ultraviolet regions radiates a large amount of energy and intensity that would contribute significantly to our electrical and chemical needs. At a power level of 1,000 Wm^{-2}, the incidence of solar energy on the earth's surface by far exceeds all human energy needs (Lewis and Nocera, 2006; Lewis et al., 2005). Against the backdrop of the

Instituto de Catálisis y Petroleoquímica (CSIC), C/Marie Curie 2, 28049, Madrid, Spain

* Corresponding author.
E-mail address: r.navarro@icp.csic.es

Advances in Chemical Engineering, Volume 36
ISSN 0065-2377, DOI: 10.1016/S0065-2377(09)00404-9

daunting carbon-neutral energy needs for sustainable development in the future, the large gap between our present use of solar energy and its enormous undeveloped potential defines a compelling imperative for science and technology in the twenty-first century. To make a material contribution to the energy supply, solar energy must be captured, converted, and stored to overcome the daily cycle and the intermittency of solar radiation. Undoubtedly, the most attractive method for this solar conversion and storage is in the form of an energy carrier such as hydrogen. The conversion of solar radiation into hydrogen offers the advantages of being transportable as well as storable for extended periods of time. This point is important because energy demand is rarely synchronous with incident solar radiation. Hydrogen is a clean energy carrier because the chemical energy stored in the H—H bond is easily released when it combines with oxygen, yielding only water as a reaction product. Accordingly, a future energy infrastructure based on hydrogen has been perceived as an ideal long-term solution to energy-related environmental problems (Bockris, 2002; Lewis and Nocera, 2006; Ogden, 2003).

The conversion of solar radiation into a chemical carrier such as hydrogen is one of the most important scientific challenges for scientists in the twenty-first century (Lewis and Nocera, 2006; Service, 2005). Solar energy can be used to produce hydrogen in the form of heat (thermochemical, Funk, 2001; Kogan et al., 2000), light (photoelectrochemical, Fujishima and Honda, 1972; photosynthetic, Miyake et al., 1999 or photocatalytic, Bard, 1980), or electricity (electrolysis, Levene and Ramsden, 2007). Solar energy used as light is the most efficient solar path to hydrogen since it does not have the inefficiencies associated with thermal transformation or with the conversion of solar energy to electricity followed by electrolysis. Therefore, the most promising method of hydrogen generation using a source of renewable energy is that based on water decomposition by means of photoelectrochemical or photocatalytic technologies using solar energy. This process mimics photosynthesis by converting water into H_2 and O_2 using inorganic semiconductors that catalyze the water-splitting reaction [Equation (1)]:

$$H_2O \rightarrow {}^{1}/_{2}O_2 + H_2\,(g) \tag{1}$$

The reaction involves the standard Gibbs free energy change (ΔG^0) greater than 237 KJ mol^{-1}, equivalent to 2.46 eV per molecule (1 eV = 96.1 KJ mol^{-1}). This energy is equivalent to the energy of photons with wavelengths shorter than 500 nm. However, direct water splitting cannot be achieved by sunlight because the water molecule cannot be electronically excited by sunlight photons (Balziani et al., 1975). Hence, appropriate systems have to be developed to efficiently absorb solar energy in order to split water in an indirect way. Since the electrochemical decomposition of water to hydrogen and oxygen is a two-electron stepwise process, it is possible to use photocatalytic surfaces capable of absorbing solar energy to generate electrons

and holes that can respectively reduce and oxidize the water molecules adsorbed on photocatalysts. The groundbreaking work of Fujishima and Honda in 1972 showed that hydrogen generation via water splitting was possible using photocatalysts based on semiconductors capable of adsorbing light energy. Since this pioneering work, there have been many papers published on the impact of different semiconductor materials on the performance in photocatalytic water splitting. These studies clearly prove that the energy conversion efficiency of water splitting is determined principally by the properties of the semiconductors used as photocatalysts. There has been significant progress in recent years in the research conducted into the development of efficient photocatalysts under visible light, but the maximum efficiency achieved up to now (2.5%) is still far from the required efficiency for practical applications. Consequently, the commercial application for hydrogen generation from solar energy and water will be determined by future progress in material science and engineering applied to the development of efficient semiconductors used as photocatalysts.

2. PHOTOELECTROCHEMISTRY OF WATER SPLITTING

2.1. Concept

Photochemical water splitting, like other photocatalytic processes, is initiated when a photosemiconductor absorbs light photons with energies greater than its band-gap energy (E_g). This absorption creates excited photoelectrons in the conduction band (CB) and holes in the valence band (VB) of the semiconductor, as schematically depicted in Figure 1a. As indicated in Figure 1b, once the photogenerated electron–hole pairs have been created in the semiconductor bulk, they must separate and migrate to the surface (paths *a* and *b* in Figure 1b) competing effectively with the electron–hole recombination process (path c in Figure 1b) that consumes the photocharges generating heat. At the surface of the semiconductor, the photoinduced electrons and holes reduce and oxidize adsorbed water to produce gaseous oxygen and hydrogen by the following reactions (described for water splitting in acid media):

$$\text{oxidation} : H_2O + 2h^+ \rightarrow 2H^+ + {}^1/_2O_2 \tag{2}$$

$$\text{reduction} : 2H^+ + 2e \rightarrow H_2 \tag{3}$$

$$\text{overall reaction} : H_2O \rightarrow H_2 + {}^1/_2O_2 \tag{4}$$

Water splitting into H_2 and O_2 is classified as an "up-hill" photocatalytic reaction because it is accompanied by a large positive change in the Gibbs free energy ($\Delta G^0 = 237\,\text{k J mol}^{-1}$, 2.46 eV per molecule). In this reaction,

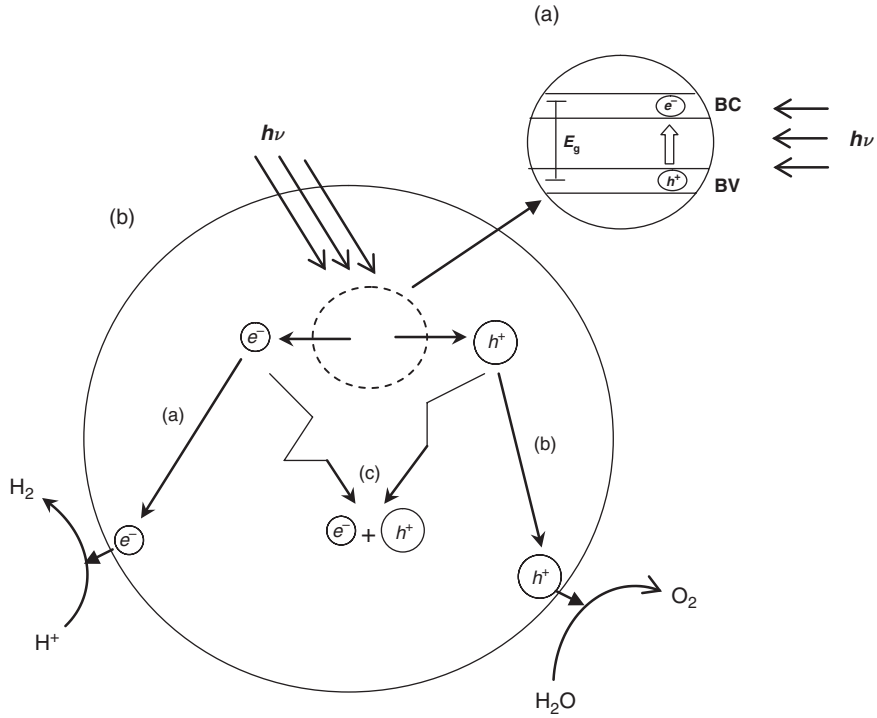

Figure 1 The principle of photocatalytic water splitting: (a) photoelectronic excitation in the phototcatalyst-generating electron–hole pairs and (b) processes occurring on photocatalyst particle following photoelectronic excitation (Mills and Le Hunte, 1997).

photon energy is converted into chemical energy (hydrogen, Figure 2), as seen in photosynthesis by green plants. This reaction is therefore sometimes referred to as artificial photosynthesis.

2.2. Configurations

Photocatalysts for photochemical water splitting can be used for this purpose according to two types of configurations: (i) photoelectrochemical cells and (ii) photocatalytic systems.

The photoelectrochemical cell for water decomposition (Figure 3) involves two electrodes immersed in an aqueous electrolyte, of which one is a photocatalyst exposed to light (photoanode in Figure 3).

The photogenerated electron–hole pairs, produced as a result of light absorption on the photoanode, are separated by an electric field within the semiconductor. On the one hand, the photogenerated holes migrate to the surface of the semiconductor where they oxidize water molecules to oxygen

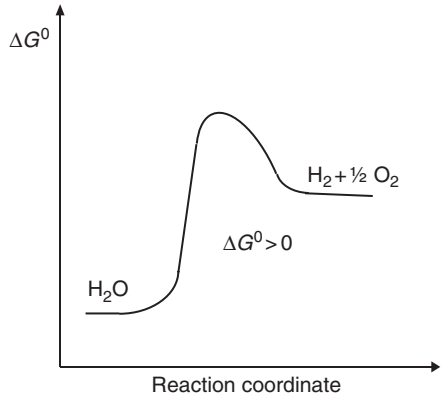

Figure 2 Change in the Gibbs free energy for water splitting (uphill reaction) (Kudo, 2003).

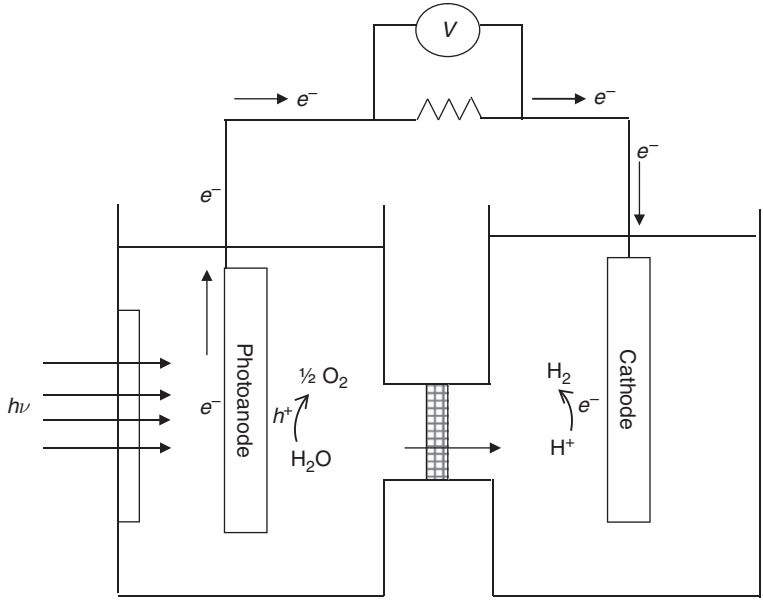

Figure 3 Diagram of photoelectrochemical cell for water splitting (Matsuoka et al., 2007).

[Equation (2)]. On the other hand, the photogenerated electrons move through an electrical circuit to the counter electrode and there reduce H^+ to hydrogen [Equation (3)]. In order to achieve practical current densities, an additional potential driving-force is usually required through the imposition of external bias voltage or the imposition of an internal bias voltage by using different concentrations of hydrogen ions in the anode/cathode compartments. Water splitting using a photoelectrochemical cell

was first reported by Fujishima and Honda (Fujishima et al., 1972, 1975) using an electrochemical system consisting of a TiO_2 semiconductor electrode connected through an electrical load to a platinum black counter electrode. Photoirradiation of the TiO_2 electrode under a small electric bias leads to the evolution of H_2 and O_2 at the surface of the Pt counter electrode and TiO_2 photoelectrode, respectively.

An alternative photoelectrochemical system is based on the use of semiconducting materials as both photoelectrodes (Nozik, 1976). In this case, n- and p-type materials are used as the photoanode and photocathode, respectively. The advantage of such a system is that photovoltages are generated on both electrodes, consequently resulting in a substantial increase in solar energy conversion and in the formation of an overall photovoltage that is sufficient for water decomposition without the application of external bias. However, the corresponding price to be paid is the concomitant increase in the device complexity derived from the fact that the photocurrents through the two electrodes must be carefully matched since the overall current flowing in the cell must obviously be the same.

The principles of photochemical water splitting can be extended to the design of systems using photocatalytic semiconductors in the form of particles or powders suspended in aqueous solutions (Bard, 1979, 1980). In this system, each photocatalyst particle functions as a microphotoelectrode performing both oxidation and reduction of water on its surface (Figure 4).

Such particulate systems have the advantage of being much simpler and less expensive to develop and use than photoelectrochemical cells. Furthermore, a wide variety of materials can be used as photocatalysts in

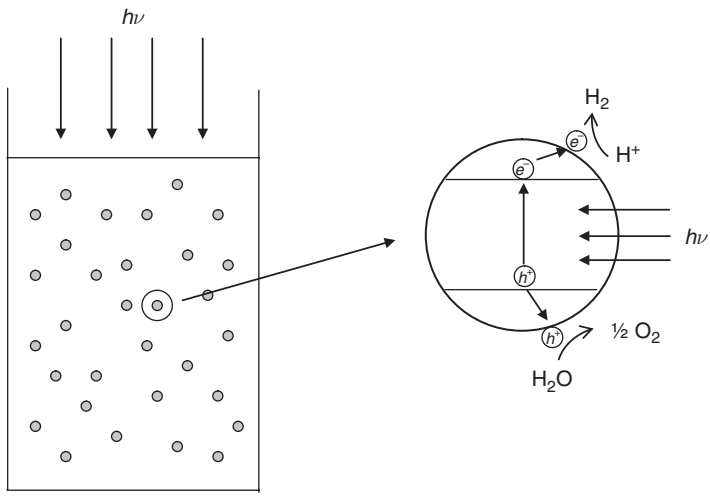

Figure 4 Scheme of the photocatalyst particulate suspension system for water splitting.

particulate systems. These particulates may be rather difficult to prepare in the form of single crystals or in form of high-quality polycrystalline phases which are necessary in the case of photoelectrodes. Another advantage is that electrical conductivity does not need to be as high as that required by photoelectrodes. Moreover, the efficiency of light absorption in suspensions or slurries of powders can be very high because of the high semiconductor surface exposed to light. For instance, 100 mg of the photocatalyst powder of particle diameter ~0.1 μm consists of more than 10^{11} particles that are mobile and independent of each other. However, particulate photocatalytic systems also have disadvantages given the separation of charge carriers is not as efficient as with a photoelectrode system, and there are difficulties associated with the effective separation of the stoichiometric mixture of oxygen and hydrogen to avoid the backward reaction.

2.3. Energy requirements

For photochemical water reduction to occur, the flat band potential of the photocatalytic semiconductor must exceed the proton reduction potential (0.0 V against the normal hydrogen electrode, NHE, at pH = 0, Figure 5). Furthermore, to facilitate water oxidation [Equation (2)], the VB edge must exceed the oxidation potential of water (+1.23 V against the NHE, at pH = 0, Figure 5). Therefore, according to these values, a theoretical semiconductor band-gap energy of 1.23 eV is required to drive the overall water-splitting reaction according to Equation (4).

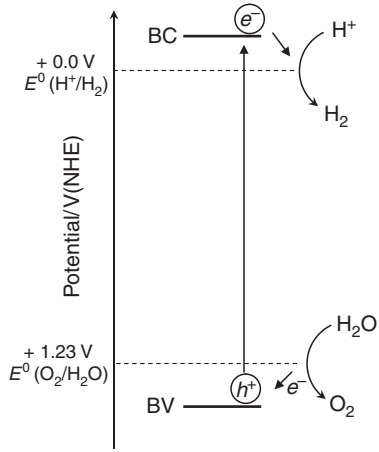

Figure 5 Potential energy diagram for photocatalytic water splitting using a single semiconductor system (Kudo, 2003).

As overall water splitting is generally difficult to achieve due to the uphill nature of the reaction, the photocatalytic activities of photocatalysts have sometimes been examined in the presence of reducing reagents (alcohols, sulfides, sulfites, EDTA) or oxidizing ones (persulfate, Ag^+, Fe^{3+} ...) to facilitate either water reduction or oxidation. The basic principle of photocatalytic reactions using redox (or sacrificial) reagents is depicted schematically in Figure 6. When the photocatalytic reaction is carried out in aqueous solutions including easily reducing reagents such as alcohols and sulfides, photogenerated holes irreversibly oxidize the reducing reagent instead of water, thus facilitating water reduction by CB electrons as shown in Figure 6a. On the other hand, electron acceptors such as Ag^+ or Fe^{3+} consume the photogenerated electrons in the CB, and the O_2 evolution reaction is enhanced as shown in Figure 6b. The reactions using redox reagents are not "overall" water-splitting reactions but are often carried out as test reactions for photocatalytic H_2 or O_2 evolution (Kato et al., 2004; Kim et al., 2004; Kudo et al., 1999; Yoshimura et al., 1993). However, one should realize that the results obtained using redox reagents do not guarantee activity for overall water splitting using pure water.

Semiconductors with band gaps smaller than 1.23 eV can be combined to drive water-oxidation/reduction processes separately via multiphoton processes. An example of this is the two-step water-splitting system using a reversible redox couple (A/R) shown in Figure 7 (Fujihara et al., 1988; Kudo et al., 1999; Sayama et al., 1987; Tennakone and Wickramanayake, 1986) with two photocatalysts with different band-gap and band

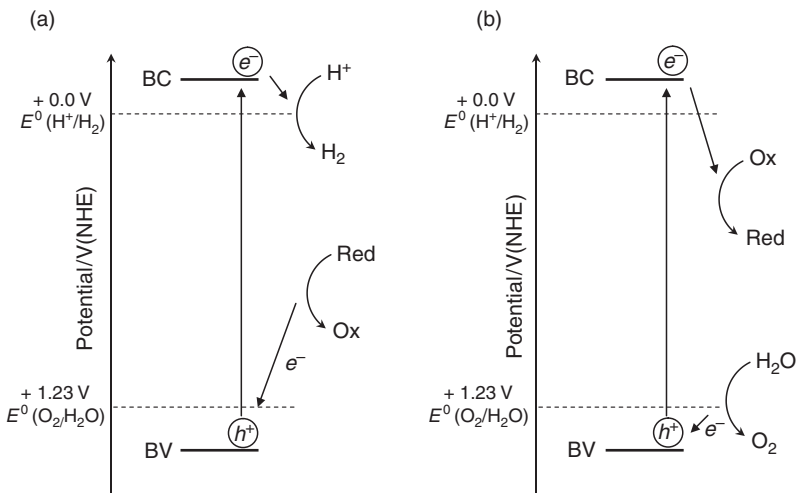

Figure 6 Schematic diagram of photocatalytic water splitting in the presence of redox (sacrificial) reagents: (a) reducing reagent (Red) for H_2 evolution and (b) oxidizing reagent (Ox) for O_2 evolution (Maeda and Domen, 2007).

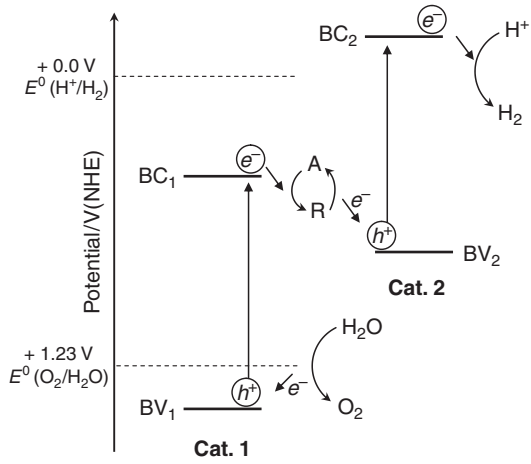

Figure 7 Diagram of a dual photocatalysts system (*z* scheme) employing a redox shuttle (Abe et al., 2005).

positions: one for O_2 evolution (cat. 1 in Figure 7) and another one for H_2 evolution (cat. 2 in Figure 7). In this two-step water-splitting configuration, water is reduced to H_2 by photoexcited electrons over the photocatalyst for H_2 evolution (cat. 2, Figure 7), and the electron donor (*R* in Figure 7) is oxidized by holes to its electron acceptor form (*A* in Figure 7). Simultaneously, this electron acceptor (*A*) is reduced to its electron donor form (*R*) by the photoexcited electrons on the photocatalyst for O_2 evolution (cat. 1 in Figure 7), while the holes on this photocatalyst oxidize water to O_2. However, the photoproduction efficiency achieved with this water-splitting configuration is low because of the use of more than one photonic processes that increase the overall energy losses associated with the light energy conversion on each photocatalysts (Tennakone and Wickramanayake, 1986).

2.4. Solar spectrum and water-splitting efficiency

The mean normal incident solar irradiance just outside the earth's atmosphere is 1353 W m^{-2} (Bird et al., 1985). The spectral distribution of sunlight that reaches the earth's surface is modified by scattering by aerosol and by absorption by ozone (in the UV region) and by water vapor and CO_2 (in the IR region). The extent of these effects depends mainly on the air mass (AM) ratio, which is the ratio between the optical path length of sunlight through the atmosphere and the path length when the sun is at the zenith.

Therefore, AM 0 sunlight means extraterrestrial sunlight, AM 1 means that the sun is overhead, and AM 25 refers to a setting or rising sun. Figure 8 shows a representative solar global spectral irradiance under the global AM

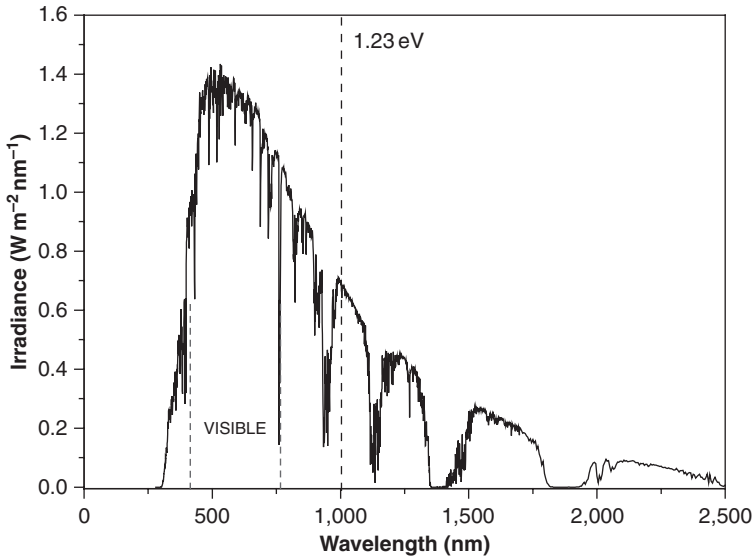

Figure 8 Solar spectral irradiance (AM 1.5) in terms of radiation energy versus photon wavelength (Bird et al., 1985).

condition 1.5 (AM 1.5). AM 1.5 corresponds to a situation when the sun is at a zenith angle of 48.19°, and it is representative of temperate latitudes in the northern hemisphere. The energy distribution in the spectrum of AM 1.5 sunlight is given in Table 1.

The efficiency to convert solar energy into chemical energy (H_2) will be the main determining factor of hydrogen production costs using photocatalyst technology. As mentioned in the previous section, the thermodynamic

Table 1 Energy distribution in the terrestrial solar spectrum (AM 1.5)

Spectral region	Interval boundaries		Solar irradiance	
	Wavelength (nm)	Energy (eV)	W m^{-2}	Percentage of total
Near UV	315–400	3.93–3.09	26	2.9
Blue	400–510	3.09–2.42	140	14.6
Green/ yellow	510–610	2.42–2.03	153	16.0
Red	610–700	2.03–1.77	132	13.8
Near IR	700–920	1.77–1.34	208	23.5
Infrared	920–> 1400	1.34 – <0.88	283	29.4

potential for water splitting requires a minimum energy of 1.23 eV per photon. This energy is equivalent to the energy of a photon with a wavelength of around 1,010 nm, and hence about 70% of all solar photons are theoretically available for water splitting (see fraction of energy above 1.23 eV in Table 1). However, all solar photonic processes involve unavoidable energy losses that in practice involve values of energy per photon higher than the theoretical limit of 1.23 eV. The energy losses associated with solar energy conversion using photocatalysts include several factors associated with the following effects: (i) transport of electrons/holes from the position of their generation at the near-surface outward to the photocatalyst–water interface; (ii) there are irreversible processes of energy loss associated with the recombination of photogenerated electron–hole pairs; (iii) all solar photons with energies lower than E_g cannot be absorbed and thus are lost to the conversion process; (iv) solar photons with energy higher than E_g can be absorbed, but the excess energy ($E_{photon} - E_g$) is lost as heat and, consequently, only a fraction of photon energy is efficiently used for conversion, and (v) the energy of the excited state in photocatalysts is thermodynamically an internal energy and not Gibbs energy [only a fraction (up to about 75%, Fonash, 1981) of the excited state energy can be used to split water].

The ideal limiting efficiency, η_{limit}, of any photonic process is given by (Archer and Bolton, 1990)

$$\eta_{limit} = \frac{J_g \Delta\mu_x \phi_c}{E_s} \tag{5}$$

where:

- J_g is the absorbed photon flux (photons s^{-1} m^{-2}) with energy higher than the band gap of the photocatalyst
- $\Delta\mu_x$ is the chemical potential of the excited state relative to the ground state of photocatalysts and represents the maximum energy available for water splitting
- Φ_c is the quantum yield (QY) of the conversion process and represents the fraction of excited states contributing to water splitting
- E_s is the total incident solar irradiance (W m^{-2}).

From Equation (5), it is clear that the basic parameter that decides the light harvesting ability of the photocatalyst is its band gap. The ideal limiting efficiencies for conversion of solar radiation calculated by Equation (5) as a function of the band-gap wavelength for standard AM 1.5 solar irradiation in a single band-gap device are represented in Figure 9.

As it can be seen in the Figure 9, the maximum ideal efficiency corresponds to semiconductors with a band-gap wavelength of $800 < \lambda_g < 950$ nm ($1.3 < E_g < 1.4$ eV). Obviously, the optimal band gap of semiconductors in terms of efficiency changes when the overall energy losses associated with

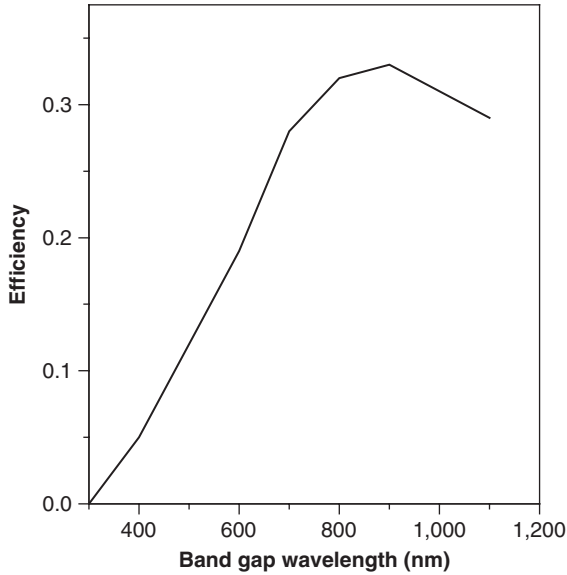

Figure 9 The ideal limiting solar conversion efficiency for a single-band gap photocatalyst (Archer and Bolton, 1990).

solar energy conversion on photocatalysts are taken into account. In this case, the efficiency, η_r, is defined according to Equation (6) (Bolton et al., 1985) to include overall energy losses:

$$\eta_r = \eta_g \phi_c \eta_{chem} \tag{6}$$

where:

-η_g is the fraction of the incident solar irradiance that has a photon energy above the photocatalyst band-gap energy. η_g is given by

$$\eta_g = \frac{J_g E_g}{E_s} \tag{7}$$

where:

-J_g is the absorbed photon flux (photons s^{-1} m^{-2}) with energy higher than the photocatalyst band-gap energy (E_g)
-E_s is the total incident solar irradiance (W m^{-2})
-η_{chem} is the chemical efficiency, that is, the fraction of the excited state energy used to split water. η_{chem} is given by

$$\eta_{chem} = \frac{E_g - E_{loss}}{E_g} \tag{8}$$

where:

- E_{loss} is the energy loss per water molecule in the photowater-splitting process. E_{loss} involves fundamental losses imposed by thermodynamics (entropy change associated with the creation of excited states) as well as losses due to nonidealities in the conversion process (transport of electron/holes, electron/holes recombination, kinetic losses, etc.). E_{loss} takes a minimum value of around 0.3–0.4 eV in ideal photocatalysts due to thermodynamic losses, and this value rises to ~0.8 eV in practical photocatalysts (Bolton, 1996).

The calculation of photoconversion efficiency by Equations (6)–(8) using a single band-gap photocatalyst and assuming a global energy loss (E_{loss}) equal to 0.8 eV gives a maximum efficiency of about 17% that is achievable with photocatalysts with optimum band-gap wavelength (λ_g) of around 600 nm (2.0–2.2 eV) (Bolton, 1996). It should be noted from Equations (6)–(8) that lowering the global energy losses in the photocatalyst (E_{loss}) augments conversion efficiency, whereby semiconductors can be used with a higher band gap (up to the limit value of $E_g \sim 1.6$ eV that corresponds to the minimum achievable thermodynamic value of $E_{loss} \sim 0.3$–0.4 eV). The above analysis has not taken into account further losses arising from incomplete absorption, QYs less than unity, reflection losses or losses in collecting gases. These losses may be estimated at around 5% according to the evaluations made by Bolton et al. (1985).

From Equations (6)–(8), it might appear that there are many factors to be determined in the measurement of solar hydrogen photoproduction efficiencies; however, in practice, efficiencies are measured using another form of Equation (6) (Serrano and de Lasa, 1997):

$$\eta_r = \frac{\Delta H^0 R_{H_2}}{E_s A} \tag{9}$$

where ΔH^0 is the standard enthalpy for water splitting, R_{H_2} is the rate of generation of H_2 (mol s^{-1}), E_s is the incident solar irradiance (W m^{-2}), and A is the irradiated area (m^2). In the case of photoelectrochemical cells, the electrical power input must be subtracted from the rate of production of the evolved hydrogen. Equation (9) must then be modified to

$$\eta_r = \frac{\Delta H^0 R_{H_2} - IV}{E_s A} \tag{10}$$

where I is the cell current (A) and V is the bias voltage applied to the cell.

3. PHOTOCATALYSTS FOR WATER SPLITTING UNDER VISIBLE LIGHT

3.1. Material requirements

Taking into account the photoelectrochemistry of water dissociation analyzed in the previous section, the photocatalysts used for the photodissociation of water must satisfy several functional requirements with respect to semiconducting and electrochemical properties: (i) suitable solar visible-light absorption capacity with a band gap of around 2.0–2.2 eV and band edge potentials suitable for overall water splitting, (ii) capacity for separating photoexcited electrons from reactive holes, (iii) minimization of energy losses related to charge transport and recombination of photoexcited charges, (iv) chemical stability against corrosion and photocorrosion in aqueous environments, (v) kinetically suitable electron transfer properties from photocatalyst surface to water, and (vi) being easy to synthesize and cheap to produce.

As stated in the previous section, the basic parameter deciding the light-harvesting ability of the photocatalyst is its electronic structure that determines the band-gap energy. Figure 10 illustrates the band positions of various semiconductors regarding the potentials (NHE) for water-oxidation/reduction processes (Xu and Schoonen, 2000).

From the perspective of band positions, among the semiconductors represented in Figure 10, those that fulfil the thermodynamic requirements for overall water splitting are $KTaO_3$, $SrTiO_3$, TiO_2, ZnS, CdS, and SiC. However, it is important to stress that the potential of the band structure

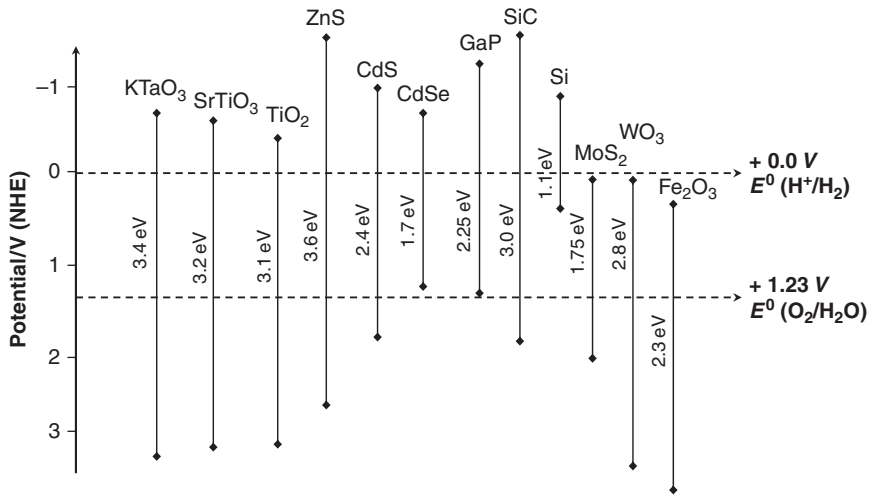

Figure 10 Band-gap energy and relative band position of different semiconductors with respect to the potentials (NHE) for water oxidation/reduction processes.

of the semiconductor is just the thermodynamic requirement. As commented in Section 1.4, there is an activation barrier in the charge transfer process between photocatalyst and water molecules derived from the energy losses associated with solar energy conversion on photocatalysts: thermodynamic losses, transport of electron/holes, electron/holes recombination, and kinetic losses. The existence of these energy losses increases the optimal band gap for high-performance photocatalysts from the theoretical value of 1.23 to 2.0–2.2 eV (Bolton, 1996).

Another essential requirement for the photocatalyst is its resistance to reactions at the solid/liquid interface that may result in a degradation of its properties. These reactions include electrochemical corrosion, photocorrosion, and dissolution (Morrison, 1980). A large group of photocatalysts with suitable semiconducting properties for solar energy conversion (CdS, GaP, etc.) are not stable in the water-oxidation reaction because the anions of these materials are more susceptible to oxidation than water, causing their degradation by oxidation of the material (Ellis et al., 1977; Williams, 1960).

Water-splitting reactions at the photocatalyst interface can occur if charge carriers generated by absorbed light can reach the solid–liquid interface during their lifetime and are capable of finding suitable reaction partners – protons for electrons and water molecules for holes. For that reason, the generation and separation of photoexcited carriers with a low recombination rate is also an essential condition to be fulfilled by the photocatalysts. The transport of photoexcited carriers strongly depends on both the microstructural and surface properties of photocatalysts. In general, the high crystalline level of the photocatalyst has a positive effect on photoactivity, as the density of defects caused by grain boundaries, which act as recombination centers of electrons and holes, decreases when particle crystallinity increases (Ikeda et al., 1997; Kominami et al., 1995; Reber and Meier, 1984). Surface properties such as surface area and active reaction sites are also important. The surface area, determined by the size of the photocatalyst particles, also influences the efficiency of charge carrier transport. To have an efficient charge transport, the diffusion length of charge carriers must be long compared to the size of the particles. Therefore, the possibility of the charge carrier reaching the surface increases as the size of the photocatalysts decreases (Ashokkumar, 1998). Nevertheless, the improvement in the efficiency associated with the high crystalline level of the photocatalyst prevails over the improvement associated with small-sized particles (Kudo et al., 2004).

3.2. Strategies for developing efficient photocatalysts under visible light

Although the properties required by photocatalysts for water splitting have been identified (band edge potentials suitable for water splitting, band-gap energy around 2.0–2.2 eV, and stability under reaction conditions), it is

difficult to obtain materials that meet all these requirements. In addition and in the development of efficient photocatalysts for water splitting, it is important to control the interinfluence between electronic, microstructural, and surface properties of photocatalysts by means of a careful design of both bulk and surface properties.

Several research approaches are pursued in the quest for more efficient and active photocatalysts for water splitting: (i) to find new single-phase materials, (ii) to tune the band-gap energy of UV-active photocatalysts (band-gap engineering), and (iii) to modify the surface of photocatalysts by deposition of cocatalysts to reduce the activation energy for gas evolution. Obviously, the previous strategies must be combined with the control of the synthesis of materials to customize the crystallinity, electronic structure, and morphology of materials at nanometric scale, as these properties have a major impact on photoactivity.

3.2.1. Band-gap engineering

In the development of active photocatalysts under visible light, it is essential to control their electronic energy structure. The strategies for controlling the energy structure of photocatalysts for water splitting may be classified in three ways: (i) cation or anion doping, (ii) use of mixed semiconductor composites, and (iii) use of semiconductor alloys.

Cation or anion doping Ion doping has been extensively investigated for enhancing the visible-light response of wide band-gap photocatalysts (UV-active). Examples include Sb- or Ta- and Cr-doped TiO_2 and $SrTiO_3$ (Kato et al., 2002; Ishii et al., 2004), ZnS doped with Cu or Ni (Kudo and Sekizawa, 1999; Kudo and Sekizawa 2000), or C-doped TiO_2 (Khan et al., 2002).

The replacement of cations in the crystal lattice of a wide band-gap semiconductor may create impurity energy levels within the band gap of the photocatalyst that facilitates absorption in the visible range, as depicted in Figure 11. Although cation-doped photocatalysts can induce visible-light response, most of these photocatalysts do not have photoactivity because dopants in the photocatalysts act not only as visible-light absorption centers, with an absorption coefficient dependent on the density of dopants, but also as recombination sites between photogenerated electrons and holes (Choi et al., 1994). Furthermore, the impurity levels created by dopants in the photocatalysts are usually discrete, which would appear disadvantageous for the migration of the photogenerated holes (Blasse et al., 1981). It is therefore important to carefully control both the content and the depth of the cation substitution in the structure of the host photocatalysts to develop visible-light-active photocatalysts. The metal ions may be incorporated into the photocatalysts by chemical methods (impregnation or precipitation) or using the advanced ion-implantation technique [based on the incorporation

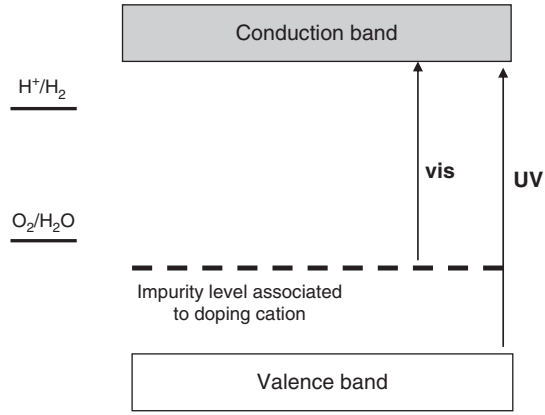

Figure 11 Band structure of cation-doped photocatalyst with visible light response from a semiconductor with wide band gap (UV response) (Kudo, 2003).

of cations by the impact of high-energy ions accelerated by high voltage (50–200 keV)] (Anpo, 2000; Anpo and Takeuchi, 2003; Yamashita et al., 2002)). The advanced ion-implantation technique is more effective than chemical methods for controlling the insertion of dopants into the photocatalyst structure (Anpo, 2000).

Anion doping is another way of enhancing the visible-light response of wide band-gap (UV-active) photocatalysts based on oxide semiconductors. In wide band-gap oxide photocatalysts, the top of the VBs consists of O 2p atomic orbitals. In recent years, interesting papers have been published on the development of visible-light photocatalysts by doping with anions such as N (Asahi et al., 2001; Hitoki et al., 2002), S (Umebayashi et al., 2002), or C (Khan et al., 2002) as substitutes for oxygen in the oxide lattice. In these anion-doped photocatalysts, the mixing of the p states of the doped anion (N, S, or C) with the O 2p states shifts the VB edge upward and narrows the band-gap energy of the photocatalyst as depicted in Figure 12. In contrast to the cationic dopant technique, the anionic replacement usually forms fewer recombination centers, and therefore, it is more effective for enhancing photocatalyst activity. Nevertheless, in the anion-doped materials, it is necessary to control the number of oxygen defects due to the difference in the formal oxidation numbers of oxygen and the dopant anions, as these defects will act as recombination centers that may reduce the efficiency of the anion-doped photocatalyst.

Composite semiconductors Semiconductor mixing (composite) is another strategy for developing photocatalysts with visible-light response from photocatalysts with a wide band gap. This strategy is based on the coupling of a wide band-gap semiconductor with a narrow band semiconductor with

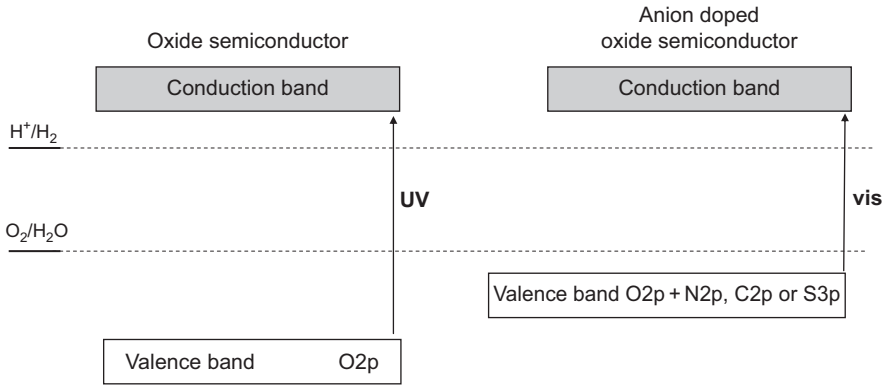

Figure 12 Band structure of anion-doped semiconductor with visible light response from a semiconductor with wide band gap (UV response) (Kudo et al., 2004).

a more negative CB level. In this way, CB electrons can be injected from the small band-gap semiconductor into the large band semiconductor, thereby extending the absorption capacity of the mixed photocatalyst (Figure 13).

An additional incentive for using composite semiconductor photocatalysts derives from the possibility of mitigating the carrier recombination by means of the interparticle electron transfer. In the photocatalyst composites, the semiconductor particles are in electronic contact with no mixing at molecular level. Illustrative examples of this approach include the following composites: CdS—TiO_2 (Serpone et al., 1984), CdS—$K_4Nb_6O_{17}$ (Yoshimura et al., 1988), or $Ca_2Fe_2O_4$—$PbBi_2Nb_{1.9}W_{0.1}O_9$ (Sung Lee, 2005).

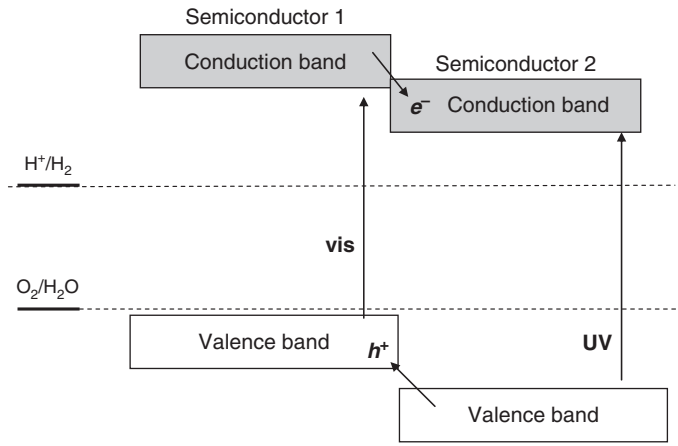

Figure 13 Band structure of the photocatalyst composite with enhanced visible-light response made from the mixture between wide and narrow band-gap photocatalysts.

The following conditions need to be met for the successful coupling of semiconductors: (i) the CB level of the semiconductor of the narrow band gap should be more negative than that of the semiconductor with a wide band gap, (ii) the CB level of the semiconductor with a wide band gap should be more negative than the water reduction potential, and (iii) electron injection should be fast and efficient.

Semiconductor alloys The third approach to the extension of the visible-light response of wide band-gap photocatalysts involves making solid solutions between wide and narrow band-gap semiconductors with a similar lattice structure as depicted in Figure 14.

Solid solutions of two or more semiconductors are formed where the lattice sites are interdispersed with the solid solution components. In these systems, the band gap can be customized by means of changes in the solid solution composition. Examples of semiconductor alloys include GaN—ZnO (Maeda et al., 2005) ZnO-GeO (Domen and Yashima, 2007), ZnS—CdS (Kakuta et al., 1985), ZnS—$AgInS_2$ (Tsuji et al., 2004), and CdS—CdSe (Kambe et al., 1984).

3.2.2. Surface modification by deposition of cocatalysts

The deposition of noble metals (e.g., Pt, Rh) or metal oxides (e.g., NiO, RuO_2) onto photocatalyst surfaces is an effective way of enhancing photocatalyst activity (Sato and White, 1980; Subramanian et al., 2001). The cocatalyst improves the efficiency of photocatalysts, as shown in Figure 15, as a result of (i) the capture of CB electrons or VB holes from the photocatalysts (Maruthamuthu and Ashokkumar, 1988), thereby reducing the possibility of electron–hole recombination and (ii) the transference

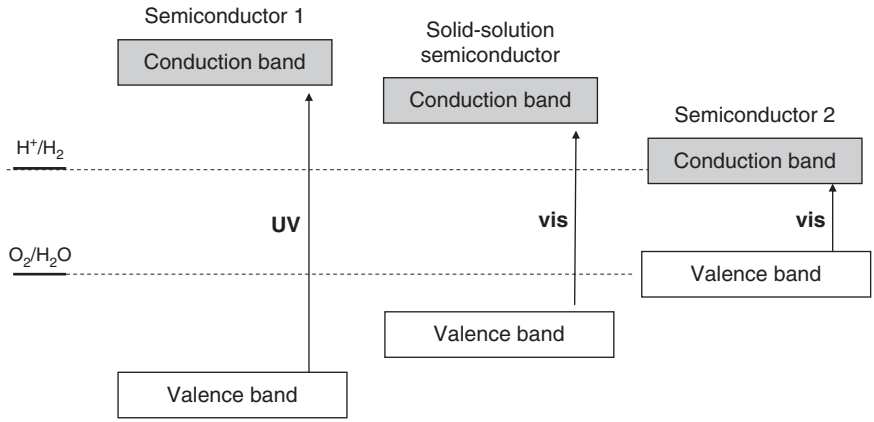

Figure 14 Band structure of photocatalysts made from the solid solution of wide and narrow band-gap photocatalysts (Kudo et al., 2004).

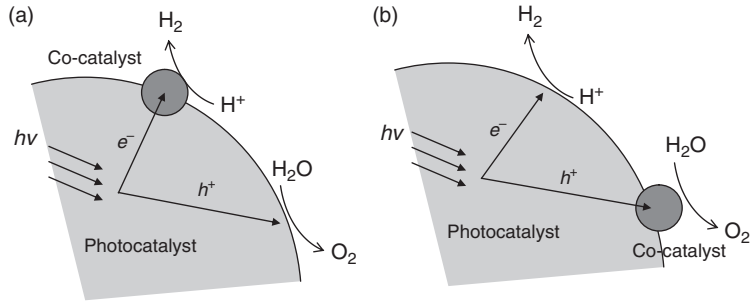

Figure 15 Schematic diagram of photocatalyst surface modification by the addition of cocatalyst to facilitate the hydrogen (a) or oxygen (b) evolution in water splitting.

of electrons and holes to surface water molecules, thereby reducing the activation energy for the reduction/oxidation of water (Maruthamuthu and Ashokkumar, 1989). The activity of the cocatalysts is found to be strongly dependent on the quantity of cocatalysts deposited on the photocatalyst surface. When the amount exceeds a critical limit, the cocatalysts act as electron–hole recombination centers, reducing the efficiency of the host photocatalyst.

3.3. Photocatalyst development

Several types of materials, over 130 including oxides, nitrides, sulfides, and others have been reported to act as efficient photocatalysts for hydrogen evolution via water splitting.

Among these photocatalysts, the higher QYs are reported for Ba-doped $Sr_2Nb_2O_7$ (50% QY, pure water, UV light) (Kim et al., 2005) and NiO/$NaTaO_3$ (56% QY, pure water UV light) (Kato et al., 2003). Unfortunately, these exciting developments have only a limited value for practical hydrogen production because UV light accounts for only about 3–4% of solar radiation energy (Table 1). Therefore, regarding the use of solar energy, it is essential to develop photocatalysts that split water efficiently under visible light ($\lambda \sim 600$ nm, Section 1.4). The materials for visible-light-driven photocatalysts had been quite limited. However, many oxides, sulfides, oxynitrides, and oxysulfides have recently been found to be active for H_2 and O_2 evolution under visible-light irradiation (Table 2). So far, the maximum quantum efficiency over visible-light-driven photocatalysts achieves only a few percent at wavelengths as long as 500 nm (Cr/Rh—GaN/ZnO 2.5% QY, pure water, visible light) (Maeda et al., 2006a). This value is still far from the QY of 10% marked as the initial starting point for practical application (Turner et al., 2008). Hence, the development of new photocatalyst materials is still a major issue. As commented in the previous section, several approaches have been adopted in

Table 2 Overview of photocatalysts developed in last years for water splitting reaction under visible light

Photocatalysts (reference)	Band-gap energy (eV)	Cocatalyst	Sacrificial reagent	Activity μmol h^{-1} g^{-1}	
				H_2	O_2
Titanium oxide and titanates					
TiO_2—Cr—Sb (Kato and Kudo, 2002)	2.2	–	$AgNO_3$ (0.05 M)		89
TiO_2—N (Kim et al., 2004)	2.73	Pt	CH_3OH (0.1 M)	0	
			$AgNO_3$ (0.05 M)		221
$SrTiO_3$—Cr—Ta (Ishii et al., 2004)	2.3	Pt	CH_3OH (0.1 M)	140	
$SrTiO_3$—Cr—Sb (Kato and Kudo, 2002)	2.4	Pt	CH_3OH (0.1 M)	156	
$La_2Ti_2O_7$—Cr (Hwang et al., 2005)	1.8–2.3	Pt	CH_3OH (0.3 M)	30	
$La_2Ti_2O_7$—Fe (Hwang et al., 2005)	1.8–2.3	Pt	CH_3OH (0.3 M)	20	
$Sm_2Ti_2S_2O_5$ (Ishikawa et al., 2002)		Pt	CH_3OH (0.3 M)	40	
		–	$AgNO_3$ (0.01 M)		16
Tantalates and niobiates					
TaON (Hitoki et al., 2002)	2.5	Pt	CH_3OH (0.06 M)	50	
		–	$AgNO_3$ (0.01 M)		3,300
$CaTaO_2N$ (Yamashita et al., 2004)	2.4	Pt	CH_3OH (0.06 M)	37	
		–	$AgNO_3$ (0.01 M)		0
$SrTaO_2N$ (Yamashita et al., 2004)	2.1	Pt	CH_3OH (0.06 M)	50	
		–	$AgNO_3$ (0.01 M)		0
$BaTaO_2N$ (Yamashita et al., 2004)	1.9	Pt	CH_3OH (0.06 M)	37	
		–	$AgNO_3$ (0.01 M)		0
$Sr_2Nb_2O_{7-x}N_x$ (Ji et al., 2005)	2.1	Pt	CH_3OH (0.14 M)	80	
		–	$AgNO_3$ (0.01 M)		8

Table 2 (*Continued*)

Photocatalysts (reference)	Band-gap energy (eV)	Cocatalyst	Sacrificial reagent	Activity μmol h^{-1} g^{-1}	
				H_2	O_2
Other transition metal oxides					
$BiVO_4$ (Kudo et al., 1998)	2.4		CH_3OH (0.1 M)	0	
		–	$AgNO_3$ (0.05 M)		421
Ag_3VO_4 (Konta et al., 2003)	2.0	–	CH_3OH (0.1 M)	0	
		–	$AgNO_3$ (0.05 M)		17
Metal oxynitrides		–			
$(Ga_{1-x}Zn_x)(N_{1-x}O_x)$ (Maeda et al., 2006)	2.4–2.8	Cr/Rh	–	930	466
$(Zn_{1+x}Ge)(N_2O_x)$ (Lee et al., 2007)	2.7	RuO_2	–	65	35
Metal sulfides					
CdS (Navarro et al., 2008)	2.4	–	S^{2-}(0.1 M)/SO_3^{2-} (0.04 M)	9.8	
CdS-CdO-ZnO (Navarro et al., 2008)	2.3	–	S^{2-}(0.1 M)/SO_3^{2-} (0.04 M)	11.6	
$Cd_{0.7}Zn_{0.3}S$ (del Valle et al., 2008)	2.68	–	S^{2-}(0.1 M)/SO_3^{2-} (0.04 M)	350	
CdS (Bühler et al., 1984)	2.4	Pt	S^{2-}(0.42 M)	34	
ZnS—Cu (Kudo and Sekizawa, 1999)	2.5	–	SO_3^{2-}(0.5 M)	450	
ZnS—Ni (Kudo and Sekizawa, 2000)	2.3	–	S^{2-}(0.005 M)/SO_3^{2-} (0.5 M)	280	

ZnS—Pb (Tsuji and Kudo, 2003)	2.3	–	S^{2-}(0.005 M)/SO_3^{2-} (0.5 M)	40	
$(AgIn)_xZn_2(1-x)S_2$ (Kudo et al., 2002)	2.4	Pt	S^{2-}(0.35 M)/SO_3^{2-} (0.25 M)	3,133	
		Pt	–	116	–
$(CuIn)_xZn_2(1-x)S_2$ (Tsuji et al., 2005)			S^{2-}(0.35 M)/SO_3^{2-} (0.25 M)		
	2.35	Ru	S^{2-}(0.35 M)/SO_3^{2-} (0.25 M)	4,000	
$(CuAg\ In)_xZn_2(1-x)S_2$ (Tsuji et al., 2005)	2.4	Ru	S^{2-}(0.5 M)	7,666	
$Na_{14}In_{17}Cu_3S_{35}$ (Zheng et al., 2005)	2.0	–		18	

the search for photocatalysts for splitting water under visible-light irradiation: (i) find new materials, (ii) tune band-gap energy by modifying UV-active photocatalysts with cation/anion doping, and (iii) manufacture a multicomponent photocatalyst by forming solid solutions. The following sections will review the above approaches for the development of active visible-light photocatalysts for water splitting.

3.3.1. Titanium oxide and titanates

Titanium oxide (TiO_2) was the first material described as a photochemical water-splitting catalyst (Fujishima and Honda, 1972). However, TiO_2 oxide photocatalyst is unable to split water under visible light. This is mainly due to the large band gap of TiO_2 (3.1 eV), which allows solely for the use of a small fraction of the solar spectrum (UV fraction). Intensive studies have been carried out to improve the visible-light sensitivity of Ti oxide-based catalysts. One of the strategies for inducing visible-light response in TiO_2 was the chemical doping of TiO_2 with metal ions with partially filled d-orbitals (V, Cr, Fe, Co, Ni, etc.) (Hwang et al., 2005; Konta et al., 2004;). Although TiO_2 chemically doped with metal ions induces a visible-light response, no significant reactivity for water splitting under visible light was described for these doped TiO_2 photocatalysts. However, Kato and Kudo (2002) reported that TiO_2 codoped with a combination of Sb^{5+} and Cr^{3+} is active for O_2 evolution under visible-light irradiation ($\lambda > 440$ nm) from an aqueous solution using $AgNO_3$ as sacrificial reagent. In this system, doped Cr^{3+} ions form an electron donor level within the band gap of TiO_2 that enables this semiconductor to absorb visible light. Codoping with Sb^{5+} was necessary to maintain the charge balance, resulting in the suppression of the formation of Cr^{6+} ions and oxygen defects in the lattice.

The physical doping of transition metal ions into TiO_2 by the advanced ion-implantation technique has been shown to enable modified TiO_2 to work under visible light (Anpo, 2000; Anpo and Takeuchi, 2003). Thin TiO_2 films implanted with metal ions such as Cr^{3+} or V^{5+} are photoactive under visible light for H_2 evolution from an aqueous solution involving methanol as sacrificial reagent with a QY of 1.25 (Matsuoka et al., 2007). Although the ion-implantation method provides a way of modifying the optical properties of TiO_2, it was impractical for mass production due to the high cost of the ion-implantation apparatus used to develop these TiO_2-modified photocatalysts.

Another strategy followed to improve the visible-light response of TiO_2 involves the doping of anions such as N (Asahi et al., 2001), S (Umebayashi et al., 2002), or C (Khan et al., 2002) as substitutes for oxygen in the TiO_2 lattice. For these anion-doped TiO_2 photocatalysts, the mixing of the p states of doped anion (S, N or C) with the O 2p states shifts the VB edge upward and narrows the band-gap energy of TiO_2. Of these materials, only N-doped TiO_2 has been tested for photocatalytic water splitting (Kim et al., 2004).

Under visible light, this Pt-modified photocatalyst evolves O_2 from aqueous $AgNO_3$ as sacrificial electron acceptor and traces of H_2 from aqueous solutions of methanol as sacrificial electron donor.

When TiO_2 is fused with metal oxides (SrO, BaO, La_2O_3, Sm_2O_3), metal titanates with intermediate band gaps are obtained. Among these titanates, attention has been paid to $SrTiO_3$, $La_2Ti_2O_7$, and $Sm_2Ti_2O_7$. $SrTiO_3$ crystallizes in the perovskite structure and has a band gap of 3.2 eV, while La_2TiO_7 is a layered perovskite with a band gap of 3.8 eV. Neither of these titanates is active under visible light because of their wide band gap. The doping of foreign metal ions into $SrTiO_3$ and La_2TiO_7 is a conventional method for the development of visible-light-driven photocatalysts based on these titanates. A survey of dopants for $SrTiO_3$ revealed that the doping of Rh or the codoping of Cr^{3+}—Ta^{5+} or Cr^{3+}—Sb^{5+} were effective in making $SrTiO_3$ visible-light-responsive (Ishii et al., 2004; Kato and Kudo, 2002; Konta et al., 2004). These doped $SrTiO_3$ samples loaded with Pt cocatalysts have recorded activity for H_2 production from aqueous methanol solutions under visible-light irradiation. On the other hand, the doping of $La_2Ti_2O_7$ with Cr^{3+} or Fe^{3+} ions allows for visible-light absorption above 400 nm of the doped-$LaTi_2O_7$ samples by exciting the electrons in the Cr 3d or Fe 3d band to the CB (Hwang et al., 2004, 2005). However, these doped $La_2Ti_2O_7$ samples have no activity for pure water splitting under visible-light irradiation. The doped $La_2Ti_2O_7$ samples are active for H_2 evolution under visible light solely in the presence of methanol as sacrificial electron donor. Another strategy followed to improve the visible-light response of layered $Ln_2Ti_2O_7$ is related to the partial substitution of oxygen by sulfur anions in the $Ln_2Ti_2O_7$ lattice. For example, promising results have been reported for $Sm_2Ti_2S_2O_5$, which has been proven to be responsive to visible-light excitation at wavelengths up to 650 nm (Ishikawa et al., 2002). S 3p atomic orbitals constitute the upper part of the VB of $Sm_2Ti_2S_2O_5$ and make an essential contribution to lowering the band-gap energy (2.0 eV) from that of the corresponding $Sm_2Ti_2O_7$ (3.5 eV). Under visible-light irradiation, the $Sm_2Ti_2S_2O_5$ works as a stable photocatalyst for the reduction of H^+ to H_2 or oxidation of H_2O to O_2 in the presence of a sacrificial electron donor (Na_2S—Na_2SO_3 or methanol) or acceptor (Ag^+).

3.3.2. Tantalates and niobates

Oxides with structural regularities such as layered and tunneling structures are considered promising materials for efficient water photodecomposition. According to this fact, tantalate and niobate oxides with corner-sharing of MO_6 (M = Ta, Nb) octahedral structure have been considered as photocatalysts for water splitting. Tantalate and niobate oxides are highly active for pure water splitting even without cocatalysts but only under UV light because of their high-energy band gap (4.0–4.7 eV) (Kato and Kudo 1999, 2001; Kato et al., 2003; Kim et al., 2005; Takata et al., 1998). The high activity

of these layered compounds is related to the easy migration and separation of the photogenerated electron–holes through the corner-shared framework of MO_6 units (Takata et al., 1998).

One way of increasing the visible response of photocatalysts based on tantalates and niobates is to form oxynitride compounds to reduce the band gap of the materials. O atoms in these compounds are partially substituted by N atoms in metal oxide causing the VB to shift to higher potential energy as a result of the hybridization of the O 2p orbitals with the N 2p orbitals. Following this strategy, $MTaO_2N$ (M = Ca, Sr, Ba), TaON, and $Sr_2Nb_2O_{7-x}N_x$ ($x = 1.5$–2.8) have been studied as photocatalysts for water splitting under visible-light irradiation (Hitoki et al., 2002; Ji et al., 2005; Yamashita et al., 2004). TaON and MTa_2N (M = Ca, Sr, Ba) have small band energies (TaON:2.5 eV, $MTaO_2N$: 2.5–2.0 eV) and are capable of absorbing visible light at 500–630 nm (Yamashita et al., 2004). TaON samples have photocatalytic activity under visible light for H_2 production from aqueous solutions using methanol as sacrificial reagent and also for O_2 production from aqueous solutions with $AgNO_3$ as electron acceptor. On the other hand, $MTaO_2N$ samples are capable of producing H_2 under visible light in the presence of methanol as sacrificial electron donor, whereas they did not have sufficient potential to oxidize water using $AgNO_3$ as electron acceptor.

Nitrogen substitution on $Sr_2Nb_2O_7$ oxides also enables the absorption of the oxynitride in the visible range as a result of the mixing of N 2p with O 2p states near the VB. $Sr_2Nb_2O_{7-x}N_x$ samples with different N substitution ($x = 1.5$–2.8) have photocatalytic activity under visible light for H_2 evolution from aqueous methanol solutions (Ji et al., 2005). The most active photocatalysts were those that achieve the higher nitrogen substitution while maintaining the original layered structure of $Sr_2Nb_2O_7$. An excess of nitrogen substitution facilitates the collapse of the layered structure of the parent oxide and turns into the less active unlayered $SrNbO_2N$.

3.3.3. Other transition metal oxides

$BiVO_4$ with scheelite structure and Ag_3VO_4 with perovskite structure were found to record photocatalytic activities for O_2 evolution from an aqueous silver nitrate solution under visible-light irradiation (Kudo et al., 1998, 1999; Konta et al., 2003). These oxides have steep absorption edges in the visible-light region. The steep edges indicate that the visible-light absorption of these oxides is due to a band–band transition. In contrast to other oxides, the VBs of $BiVO_4$ and Ag_3VO_4 consist of Bi and Ag orbitals mixed with O 2p states that result in an increase in VB potentials and a decrease in band-gap energy. This enables $BiVO_4$ and Ag_3VO_4 to absorb visible light. However, these catalysts had no potential for H_2 production because the CB potentials of the photocatalysts do not have sufficient overpotential for the reduction potential of water.

3.3.4. Metal (oxy) nitrides

The nitrides and oxynitrides of transition metal-cations with d^{10} electronic configuration (Ga^{3+}, Ge^{4+}) are a new type of photocatalysts that can split pure water under visible light without sacrificial reagents. In the development of oxynitride with d^{10} electronic configuration, the solid solution between GaN and ZnO ($(Ga_{1-x}Zn_x)(N_{1-x}O_x)$) was tested first (Maeda et al., Maeda et al., 2005a; Maeda et al., 2005b). GaN and ZnO have wurtzite structures with similar lattice parameters and can therefore form solid solutions. While GaN and ZnO have band-gap energies greater than 3 eV and therefore do not absorb visible light, the $(Ga_{1-x}Zn_x)(N_{1-x}O_x)$ solid solution has absorption edges in the visible region with band energies of 2.4–2.8 eV. Density functional calculations indicated that the visible-light response of the solid solution originates from the presence of Zn 3d and N 2p electrons in the upper VB that provide p–d repulsion for the VB, resulting in the narrowing of the band gap. The $(Ga_{1-x}Zn_x)(N_{1-x}O_x)$ solid solution has low photocatalytic activity even under UV irradiation. However, its activity under visible light increases remarkably with the modification of $(Ga_{1-x}Zn_x)(N_{1-x}O_x)$ solid solution by superficial deposition of cocatalyst nanoparticles. Different transition metals and oxides have been examined as cocatalysts to promote the activity of $(Ga_{1-x}Zn_x)(N_{1-x}O_x)$ solid solutions (Maeda et al., 2006a, b). Among the various cocatalysts examined, the largest improvement in activity was obtained when $(Ga_{1-x}Zn_x)(N_{1-x}O_x)$ was loaded with a mixed oxide of Rh and Cr. From this sample, it is observed that H_2 and O_2 evolve steadily and stoichiometrically under visible light from pure water without sacrificial reagents. The quantum efficiency of the Rh-Cr-loaded $(Ga_{1-x}Zn_x)(N_{1-x}O_x)$ photocatalyst for overall water splitting reaches ca. 2.5% at 420–440 nm (Maeda et al., 2005). These photocatalysts based on $(Ga_{1-x}Zn_x)(N_{1-x}O_x)$ solid solutions were the first particulate photocatalyst systems capable of performing overall water splitting by one-step photoexcitation under visible light.

The solid solution between ZnO and $ZnGeN_2$ ($(Zn_{1+x}Ge)(N_2O_x)$) has also been found to be an active oxynitride photocatalyst for pure water splitting under visible light (Lee et al., 2007). The solid solutions $(Zn_{1+x}Ge)(N_2O_x)$ present absorption in the visible region with a band-gap energy of ca. 2.7 eV, which is smaller than the band gaps of Ge_3N_4 (3.8 eV), $ZnGeN_2$ (3.3 eV), and ZnO (3.2 eV). The visible-light response of this material originates from the p–d repulsion between Zn 3d and N 2p and O 2p electrons in the upper part of the VBs that narrows the band gap. Neither $ZnGeN_2$ nor ZnO alone exhibits photocatalytic activity for overall water splitting under UV irradiation. However, the solid solution $(Zn_{1+x}Ge)(N_2O_x)$ loaded with nanoparticulate RuO_2 cocatalyst becomes active under visible-light irradiation generating H_2 and O_2 stoichiometrically from pure water.

3.3.5. Metal sulfides

Sulfide photocatalysts, which have a narrow band gap and VBs at relatively negative potentials compared to oxides, are good candidates for visible-light-driven photocatalysts. Metal sulfide photocatalysts, however, are not stable in the water-oxidation reaction under visible light because the S^{2-} anions are more susceptible to oxidation than water, thereby causing the photodegradation of the photocatalyst (Ellis et al., 1977; Williams, 1960). For this reason, sulfide photocatalysts are not suitable for water splitting unless appropriate strategies are designed to minimize photodegradation. A common method for reducing the photocorrosion of the sulfides under irradiation is by means of the use of suitable sacrificial reagents. Photocorrosion may be effectively suppressed by using a Na_2S/Na_2SO_3 mixture as electron donor (Reber and Meier, 1986). Using this mixed solution, the photocatalytic reaction should proceed as follows, avoiding the degradation of the sulfide photocatalyst:

$$\text{Photocatalysts} + h\nu \rightarrow e^-(\text{CB}) + h^+(\text{VB})$$

$$2H_2O + 2e^-(\text{CB}) \rightarrow H_2 + 2OH^-$$

$$SO_3^{2-} + H_2O + 2h^+(\text{VB}) \rightarrow SO_4^{2-} + 2H^{++}$$

$$2S^{2-} + 2h + (\text{VB}) \rightarrow S2^{2-}$$

$$S_2^{2-} + SO_3^{2-} \rightarrow S_2O_3^{2-} + S^{2-}$$

$$SO_3^{2-} + S^{2-} + 2h + (\text{VB}) \rightarrow S_2O_3^{2-}$$

Among the available sulfide semiconductors, nanosized CdS is an interesting photocatalyst material, since it has a narrow band gap (2.4 eV) and a suitable CB potential to effectively reduce the H^+ (Darwent and Porter, 1981; Matsumura et al., 1983; Reber and Meier, 1986). CdS loaded with Pt cocatalyst records a very high efficiency in light absorption and hydrogen production under visible light (QE = 25%, Bühler et al., 1984). However, the photocatalytic properties of CdS are limited as a consequence of its toxicity and photocorrosion under visible-light irradiation. In spite of the drawbacks associated with CdS, considerable efforts are still being made to improve its photocatalytic properties. The strategies reported in the technical literature to improve the activity of CdS include (i) changes in the structural characteristics of CdS and (ii) the combination of CdS with different elements or semiconductors to form composite photocatalysts with tuned band-gap size.

Considering the importance of the structural characteristics (crystalline phase, crystalline size, and geometrical surface area) in the control of band structure and in the concentration and mobility of photocatalyst charges, studies have been conducted on the influence of preparation methods on the photophysical properties of CdS (Arora et al., 1998; Jing and Guo, 2006). Improvement in CdS photoactivity is observed from preparation methods that lead to CdS phases with good crystallinity and few crystal defects.

Changes in the photoactivity of CdS can also be achieved by combining the CdS with other semiconductors with different energy levels: ZnO (Navarro et al., 2008; Spanhel et al., 1987) or TiO_2 (Fujii et al., 1998). In these composite systems, photogenerated electrons move from CdS to the attached semiconductors, while photogenerated holes remain in CdS. This charge-carrier separation stops charge recombination, thereby improving the photocatalytic activity of CdS. Improvements in CdS activity are reported for samples mixed with CdO and ZnO (Navarro et al., 2008). This improvement was linked to the better charge separation associated with the diffusion of photoelectrons generated in CdS toward surrounding CdO and ZnO. The incorporation of elements in the structure of CdS to make a solid solution is another strategy for improving the photocatalytic properties of CdS. ZnS is interesting as a semiconductor for combining with CdS. CdS and ZnS form a continuous series of solid solutions ($Cd_{1-x}Zn_xS$) where metal atoms are mutually substituted in the same crystal lattice (Fedorov et al., 1993; Nayeem et al., 2001). Valle et al. (2008) investigated the photophysical and photocatalytic properties of $Cd_{1-x}Zn_xS$ solid solutions with different Zn concentration ($0.2 < x < 0.35$). The solid solution between CdS and ZnS showed a blue shift of the absorption edge with the increase in Zn concentration. The photocatalytic activity of samples increases gradually when the Zn concentration increases from 0.2 to 0.3. The change in activity for H_2 production for these samples arises mainly from the modification of the energy level of the CB as the concentration of Zn increased in the solid solution photocatalyst.

ZnS is another sulfide semiconductor that has been investigated for photochemical water splitting. ZnS is unable to split water under visible light because of its large band gap (3.66 eV), which restricts light absorption to the UV region. Studies have been carried out to improve the visible-light sensitivity of ZnS-based photocatalysts. One of the strategies for inducing visible-light response in ZnS was the chemical doping of ZnS with metal ions: Cu^{2+} (Kudo and Sekizawa, 1999), Ni^{2+} (Kudo and Sekizawa, 2000), and Pb^{2+} (Tsuji and Kudo, 2003). The doped ZnS materials are capable of absorbing visible light as a result of the transitions from M^{n+} (M = Cu, Ni, Pb) levels to the CB of ZnS. These doped ZnS photocatalysts had high photocatalytic activity under visible light for H_2 production from aqueous solutions using SO_3^{2-}/S^{2-} as electron donor reagents.

A combination of ZnS with $AgInS_2$ and $CuInS_2$ to produce solid solutions $(CuAgIn)_xZn_{2(1-x)}S_2$ is another strategy followed to improve the optical absorption of ZnS in the visible range (Kudo et al., 2002; Tsuji et al., 2005a, b). The optical adsorption of these materials can be adjusted between 400 and 800 nm depending on solid solution composition. $(CuAgIn)_xZn_{2(1-x)}S_2$ solid solutions recorded high photocatalytic activities for H_2 evolution from aqueous solutions containing sacrificial reagents, SO_3^{2-} and S^{2-}, under visible-light irradiation. Loading solid solutions with cocatalysts improved photocatalytic activity. Pt loaded on $(AgIn)_{0.22}Zn_{1.56}S_2$ recorded the highest activity for H_2 evolution with an apparent QY of 20% at 420 nm.

Other ternary sulfides comprising In^{3+} and one type of transition metal cation (Cd^{2+}, Zn^{2+}, Mn^{2+}, Cu^{+}) are also investigated as photocatalysts for water splitting under visible light. However, the efficiency for water splitting under visible light achieved over these photocatalysts has so far been very low. For example, a quantum efficiency of only 3.7% at 420 nm was reported for the most active $Na_{14}In_{17}Cu_3S_{35}$ photocatalyst (Zheng et al., 2005).

4. CONCLUDING REMARKS AND FUTURE DIRECTIONS

1. Solar-hydrogen production via the water-splitting reaction on photocatalyst surfaces is one of the most promising technologies for the generation of energy in a clean and sustainable manner.
2. The success of this technology will be determined by the development of efficient photocatalysts that must satisfy very specific semiconducting and electrochemical properties.
3. Since the pioneering work by Fujishima and Honda, research has made significant progress in the development of efficient photocatalysts under visible light. From these studies, it is readily apparent that the energy conversion efficiency of water splitting is determined principally by the properties of the semiconductors used as photocatalysts.
4. In spite of these progresses, current results still record low efficiencies for visible-light-to-hydrogen conversion (2.5% QY) for practical purposes (10% QY).
5. To improve the efficiency of photocatalysts, developments in the future must be based on an understanding of the sophisticated factors that determine the photoactivity of the water-splitting reaction: (i) molecular reaction mechanisms involved in the oxidation and reduction of water on photocatalyst surfaces, (ii) structure and defect chemistry of photocatalyst surfaces, and (iii) charge transfer mechanisms between

semiconductor surfaces and cocatalysts. Nowadays, these factors have not been elucidated in sufficient detail and should be investigated as a way of refining the materials to maximize efficiency. On the other hand, the search for new photocatalytic materials with improved semiconducting and electrochemical properties is still likely to be the key to success. High throughput screening or combinational chemistry approaches, as well as more rational research based on fundamental calculations/predictions, would be useful in the search for new photocatalytic materials. Finally, the control of the synthesis of materials for customizing the crystallinity, electronic structure, and morphology of photocatalysts at nanometric scale also provide significant opportunities for improving water-splitting photocatalysts, as these properties have a major impact on photoactivity.

6. Considering the advances made in UV photocatalysts since the pioneering work of Fujishima and Honda in 1972 through to the present day, technically and economically viable visible-light photocatalysts for water splitting could become available in the near future.

ACKNOWLEDGMENTS

We are grateful to many of our colleagues for stimulating discussions and to our research sponsors CICyT and CAM (Spain) under grants ENE2007-07345-C03-01/ALT and S-0505/EN/0404, respectively. JAVM acknowledges financial support from the Autonomous Community of Madrid (Spain). MCAG acknowledges financial support from the Ministry of Science and Education (Spain) through the R&C Program.

REFERENCES

Abe, R., Sayama, K., and Sughihara, H. *J. Phys. Chem. B* **109**(33), 16052 (2005).
Anpo, M. *Pure Appl. Chem.* **72**, 1265 (2000).
Anpo, M., and Takeuchi, M. *J. Catal.* **216**, 505 (2003).
Archer, M.D., and Bolton, J.R. *J. Phys. Chem.* **94**, 8028 (1990).
Arora, M.K., Shinha, A.S.K., and Updhyay, S.N. *Ind. Eng. Chem. Res.* **37**(10), 3950 (1998).
Asahi, R., Morikawa, T., Ohwaki, T., Aoki, K., and Taga, Y. *Science* **293**, 269 (2001).
Ashokkumar, M. *Int. J. Hydrogen Energy* **23**(6), 427 (1998).
Balziani, V., Moggi, L., Manfrin, M.F., Bolleta, F., and Gleria, M. *Science* **189**, 852 (1975).
Bard, A.J. *J. Photochem.* **10**, 59 (1979).
Bard, A.J. *Science* **207**, 139 (1980).
Bird, R.E., Hulstrom, R.L., and Lewis, L. *J. Solar Cell* **15**, 365 (1985).
Blasse, G., Dirksen, J., and de Korte, P.H.M. *Mater. Res. Bull.* **16**, 991 (1981).
Bockris, J.O.M. *Int. J. Hydrogen Energy* **27**, 731 (2002).
Bolton, J.R., Strickler, S.J., and Conolly, J.S. *Nature* **316**, 495 (1985).
Bolton, J.R. *Solar Energy* **57**(1), 37 (1996).
Bühler, N., Meier, K., and Reber, J.F. *J. Phys. Chem.* **88**(15), 3261 (1984).
Choi, W.Y., Termin, A., and Hoffman, M.R. *J. Phys. Chem.* **84**, 13669 (1994).
Darwent, J.R., and Porter, G. *J. Chem. Soc. Chem. Commun.* **4**, 145 (1981).

Domen, K., and Yashima, M. *J. Phys. Chem. C* **111**, 1042 (2007).
Ellis, A.B., Kaiser, S.W., Bolts, J.M., and Wrighton, M.S. *J. Am. Chem. Soc.* **99**, 2839 (1977).
Fedorov, V.A., Ganshing, V.A., and Norkeshko, Y.U.N. *Mater Res. Bull.* **28**, 50 (1993).
Fonash, S.J. "Solar Cell Device Physics". Academic Press, San Diego (1981).
Fujihara, K., Ohno, T., and Matsumura, M. *J. Chem. Soc. Faraday Trans.* **94**, 3705 (1998).
Fujii, H., Ohtaki, M., Eguchi, K., and Arai, H. *J. Mol. Catal: A Chem.* **129**(1), 61 (1998).
Fujishima, A., and Honda, K. *Nature* **238**, 37 (1972).
Fujishima, A., Kohaakawa, K., and Hond, K. *J. Electrochem. Soc.* **122**, 1487 (1975).
Funk, J. *Int. J. Hydrogen Energy* **26**, 185 (2001).
Hitoki, G., Takata, T., Kondo, J.N., Hara, M., Kobayashi, H., and Domen, K. *Chem. Commun.* **16** 1698 (2002).
Hwang, D.W., Kim, H.G., Jang, J.S., Bae, S.W., Ji, S.M., and Lee, J.S. *Catal. Today* **93**, 845 (2004).
Hwang, D.W., Kim, H.G., Lee, J.S., Kim, J., Li, W., and Oh, S.H. *J. Phys. Chem. B* **109**, 2093 (2005).
Ikeda, S. Tanaka, A., Shinohara, K., Hara, M., Kondo, J.N., Maruya, K., and Domen, K. *Microp. Mater.* **9**, 253 (1997).
Ishii, T., Kato, H., and Kudo, A. *J. Photochem. Photobiol. A* **163**, 181 (2004).
Ishikawa, A., Takata, T., Kondo, J.N., Hara, M., Kobayashi, H., and Domen, K. *J. Am. Chem. Soc.* **124**, 13547 (2002).
Ji, S.M., Borse, P.H., Kim, H.G., Hwang, D.W., Jang, J.S., Bae, S.W., and Lee, J.S. *Phys. Chem. Chem. Phys.* **7**, 1315 (2005).
Jing, D.W., and Guo, L.J. *J. Phys. Chem. B*. **110**(23), 11139 (2006).
Kakuta, N., Park, K.H., Finlayson, M.F., Ueno, A., Bard, A.J., Campion, A., Fox, M.A., Webber, S.E., and White, J.M. *J. Phys. Chem.*, **89**, 732 (1985).
Kambe, S., Fujii, M., Kawai, T., and Kawai, S. *Chem. Phys. Lett.* **109**, 105 (1984).
Kato, H., Asakura, K., and Kudo, A. *J. Am. Chem. Soc.* **125**, 3082 (2003).
Kato, H., Hori, M., Konta, R., Shimodaira, Y., and Kudo, A. *Chem. Lett.* **33**, 1348 (2004).
Kato, H., Kobayashi, H., and Kudo, A. *J. Phys. Chem. B* **106**, 12441 (2002).
Kato, H. and Kudo, A. *Chem. Lett.*, **11**, 1207, (1999).
Kato, H., and Kudo, A. *J. Phys. Chem. B* **105**, 4285 (2001).
Kato, H., and Kudo, A. *J. Phys. Chem. B* **106**, 12441 (2002).
Khan, S.U.M., Al-Shahry, M., and Ingler, W.B. *Science* **297**, 2243 (2002).
Kim, J., Hwang, D.W., Kim, H.G., Lee, J.S., Li, W., and Oh, S.H. *Topics Catal.* **35**(3–4), 295 (2005).
Kim, H.G., Hwang, D.W., and Lee, J.S. *J. Am. Chem. Soc.* **126**(29), 8912 (2004).
Kogan, A., Splieger, E., and Wolfshtein, M. *Int. J. Hydrogen Energy* **25**, 739 (2000).
Kominami, H., Matsuura, T., Iwai, K., Ohtani, B., Nishimoto, S., and Kera, Y. *Chem. Lett.* 693 (1995).
Konta, R., Ishii, T., Kato, H., and Kudo, A. *J. Phys. Chem. B* **108**, 8992, (2004).
Konta, R. Kato, H., Kobayashi, H., and Kudo, A. *Phys. Chem. Chem. Phys.* **5**, 3061 (2003)
Kudo, A. *Catal. Survey Asia* **7**(1), 31 (2003)
Kudo, A., Kato, H., and Tsuji, I. *Chem. Lett.* **33**(12), 1534 (2004).
Kudo, A., Omori, K., ana Kato, H. *J. Am. Chem. Soc.* **121**, 11459 (1999).
Kudo, A., and Sekizawa, M. *Catal. Lett.* **58**, 241 (1999).
Kudo, A., and Sekizawa, M. *Chem. Commun.* **15**, 1371 (2000)
Kudo, A., Tsuji, I., and Kato, H. *Chem. Commum.* **17**, 1958 (2002).
Kudo, A., Ueda, K., Kato, and Mikami, I. *Catal. Lett.* **53**, 229 (1998).
Levene, J., and Ramsden, T. "*Summary of Electrolytic Hydrogen Production*". National Renewable Energy Laboratory, Golden, CO, MP-560-41099, (2007).
Lewis, N.S., Crabtree, G., Nozik, A.J., Wasielewski, M.R., and Alivisatos, A.P. "Basic Reseach Needs for Solar Energy Utilization". U.S. Department of Energy, Washington, DC, (2005).
Lewis, N.S., and Nocera, D.G. *Proc. Natl. Acad. Sci. USA* **103**(43), 15729 (2006).
Maeda, K., and Domen, K. *J. Phys. Chem. C* **111**, 7851 (2007).
Maeda, K., Teramura, K., Takata, K., Hara, M., Saito, N., Toda, K., Inoue, I., Kobayashi, H., and Domen, K. *J. Phys. Chem. B* **109**(43), 20504 (2005a).

Maeda, K., Takata, T., Hara, M., Saito, M., Inoue, Y., Kobayashi, H., and Domen, K. *J. Am. Chem. Soc.* **127**, 8286 (2005b).
Maeda, K., Teramura, K., Lu, D., Takata, T., Saito, N., Inue, Y., and Domen, K. *Nature* **440**(7082), 295 (2006a).
Maeda, K., Teramura, K., Saito, N., Inoue, Y., and Domen, K. *J. Catal.* **243**, 303 (2006b).
Maruthamuthu, P., and Ashokkumar, M. *Int. J. Hydrogen Energy* **13**, 677 (1988).
Maruthamuthu, P., and Ashokkumar, M. *Int. J. Hydrogen Energy* **14**, 275 (1989).
Matsumura, M., Saho, Y., and Tsubomura, H. *J. Phys. Chem.* **87**, 3807 (1983).
Matsuoka, M., Kitano, M., Takeuchi, M., Tsujimaru, K., Anpo, M., and Thomas, J.M. *Catal. Today* **122**, 51 (2007).
Mills, A., and Le Hunte, S. *J. Photochem. Photobiol. A Chem.* **108**, 1 (1997).
Miyake, J., Miyake, M., and Adsada, Y. *J. Biotechnol.* **70**, 89 (1999).
Morrison, S.R. "Electrochemistry at Semiconductor and Oxidized Metal Electrodes". Plenum Press, New York (1980).
Navarro, R.M., del Valle, F., and Fierro, J.L.G. *Int. J. Hydrogen Energy* **33**, 4265 (2008).
Nayeem, A., Yadaiah, K., Vajralingam, G., Mahesh, P., and Nagabhooshanam, M. *Int. J. Mod. Phys. B* **15**(7), 2387 (2001).
Nozik, A.J. *Appl. Phys. Lett*. **29**, 150 (1976).
Ogden, J.M. "Testimony to the Committee on Science" US House of Representatives; Washington, DC, (2003).
Reber, J.F., and Meier, K. *J. Phys. Chem.* **88**, 5903 (1984)
Reber, J.F., and Meier, K. *J. Phys. Chem.* **90**, 824 (1986).
Sato, S., and White, J.M. *Chem. Phys. Lett.* **72**, 83 (1980).
Sayama, K., Yoshida, R., Kusama, H., Okabe, K., Abe, Y., and Arakawa, H. *Chem. Phys. Lett.* **277**, 387 (1997).
Serpone, N., Borgarelo, E., and Grätzel, M. *Chem. Comm*. 342 (1984).
Serrano, M., and de Lasa, H. *Ind. Eng. Chem. Res.* **36**, 4705 (1997)
Service, R.F. *Science* **309**, 548 (2005).
Spanhel, L., Weller, H., and Henglein, A. *J. Am. Chem. Soc.* **109**, 6632 (1987).
Subramanian, V., Wolf, E., Kamat, P.V. J. of *Phys. Chem. B*. **105**(46), 11439 (2001).
Sung Lee, J. *Catal. Survey Asia* **9**(4), 217 (2005).
Takata, T., Tanaka, A., Hara, M., Kondo, J.N., and Domen, K. *Catal. Today* **44**, 17 (1998).
Tennakone, K., and Wickramanayake, S.J. *J. Chem. Soc. Faraday Trans.* **92**(1) 1475 (1986).
Tsuji, I., Kato, H., Kobayashi, H., and Kudo, A. *J. Am. Chem. Soc.* **126**, 13406 (2004).
Tsuji, I., Kato, H., Kobayashi, H., and Kudo, A. *J. Phys. Chem. B.* **109**, 7329 (2005a).
Tsuji, I., Kato, H., and Kudo, A. *Angew. Chem. Int. Ed.* **44**, 3565 (2005b).
Tsuji, I., and Kudo, A. *J. Photochem. Photobiol. A* **156**(1–3), 249 (2003).
Turner, J., Sverdrup, G., Mann, M.K., Maness, P-C., Kroposki, B., Ghirardi, M., Ewans, R.J., Blake, D. *Int. J. of Energy Res*. **32**(5), 379 (2008).
Umebayashi, T., Yamaki, T., Itoh, H. and Asai, K. *Appl. Phys. Lett*. **81**, 454 (2002).
Valle, F., Navarro, R.M., Ishikawa, A., Domen, K., and Fierro, J.L.G. "International Symposium on Catalysis for Clean Energy and Sustainable Chemistry". Madrid, Spain (2008).
Williams, R., *J. Chem. Phys*. **32**, 1505 (1960).
Xu, Y., and Schoonen, M.A.A., *Am. Mineral.* **85**, 543 (2000).
Yamashita, H., Harada, M., Misaka, J., Takeuchi, M., Ikeue, K., and Anpo, M. *J. Photochem. Photobiol. A* **148**, 257 (2002).
Yamashita, D., Takata, T., Hara, M., Kondo, J.N., and Domen, K. *Solid State Ionics* **172**, 591 (2004)
Yoshimura, J., Ebina, Y., Kondo, J., Domen, K., and Tanaka, A. *J. Phys. Chem.* **97**, 1970 (1993)
Yoshimura, J., Kudo, A., Tanaka, A., Domen, K., Maruya, K., and Onishi, T. *Chem. Phys. Lett.* **147**, 401 (1988).
Zheng, N., Bu, X., Vu, H., and Feng, P. *Angew. Chem. Int. Ed.* **44**, 5299 (2005).